

A molecular dynamics study on mechanical performance and deformation mechanisms in nanotwinned NiCo-based alloys with nano-precipitates under high temperatures

Zihao Yu(于子皓), Hongyu Wang(王鸿宇), Ligang Sun(孙李刚), Zhihui Li(李志辉), and Linli Zhu(朱林利)

Citation: Chin. Phys. B, 2024, 33 (**11**): 116201. DOI: 10.1088/1674-1056/ad6cca
Journal homepage: http://cpb.iphy.ac.cn; http://iopscience.iop.org/cpb

What follows is a list of articles you may be interested in

Theoretical insights into the structures and fundamental properties of pnictogen nitrides

Jingjing Wang(王晶晶), Panlong Kong(孔攀龙), Dingmei Zhang(张定梅), Defang Gao(高德芳), Zaifu Jiang(蒋再富), and Wei Dai(戴伟)
Chin. Phys. B, 2024, 33 (**9**): 096201. DOI: 10.1088/1674-1056/ad6a07

Utilizing of high-pressure high-temperature synthesis to enhance the thermoelectric properties of $Zn_{0.98}Al_{0.02}O$ with excellent electrical properties

Qi Chen(陈启), Xinjian Li(李欣健), Yao Wang(王遥), Lijie Chang(常立杰), Jian Wang(王健), Yuewen Zhang(张跃文), Hongan Ma(马红安), and Xiaopeng Jia(贾晓鹏)
Chin. Phys. B, 2021, 30 (**1**): 016202. DOI: 10.1088/1674-1056/abc4dd

Synthesis of black phosphorus structured polymeric nitrogen

Ying Liu(刘影)†, Haipeng Su(苏海鹏), Caoping Niu(牛草萍), Xianlong Wang(王贤龙), Junran Zhang(张俊然), Zhongxue Ge(葛忠学), and Yanchun Li(李延春)
Chin. Phys. B, 2020, 29 (**10**): 106201. DOI: 10.1088/1674-1056/aba9bd

Nanosheet-structured B_4C with high hardness up to 42 GPa

Chang-Chun Wang(王常春), Le-Le Song(宋乐乐)
Chin. Phys. B, 2019, 28 (**6**): 066201. DOI: 10.1088/1674-1056/28/6/066201

First-principles investigations on structural stability, mechanical, and thermodynamic properties of LaT_2Al_{20} (T=Ti, V, Cr, Nb, and Ta) intermetallic cage compounds

Shanyu Quan(权善玉), Xudong Zhang(张旭东), Cong Liu(刘聪), Wei Jiang(姜伟)
Chin. Phys. B, 2018, 27 (**12**): 126201. DOI: 10.1088/1674-1056/27/12/126201

A molecular dynamics study on mechanical performance and deformation mechanisms in nanotwinned NiCo-based alloys with nano-precipitates under high temperatures

Zihao Yu(于子皓)[1], Hongyu Wang(王鸿宇)[1], Ligang Sun(孙李刚)[2], Zhihui Li(李志辉)[3,4], and Linli Zhu(朱林利)[1,†]

[1] *School of Aeronautics and Astronautics, Center for X-Mechanics, Zhejiang University, Hangzhou* 310027, *China*
[2] *School of Science, Harbin Institute of Technology, Shenzhen* 518067, *China*
[3] *Hypervelocity Aerodynamics Institute, China Aerodynamics Research and Development Center, Mianyang* 621000, *China*
[4] *National Laboratory for Computational Fluid Dynamics, Beijing* 100191, *China*

(Received 23 May 2024; revised manuscript received 4 August 2024; accepted manuscript online 8 August 2024)

Molecular dynamics simulations are performed to investigate the mechanical behavior of nanotwinned NiCo-based alloys containing coherent $L1_2$ nano-precipitates at different temperatures, as well as the interactions between the dislocations and nano-precipitates within the nanotwins. The simulation results demonstrate that both the yield stress and flow stress in the nanotwinned NiCo-based alloys with nano-precipitates decrease as the temperature rises, because the higher temperatures lead to the generation of more defects during yielding and lower dislocation density during plastic deformation. Moreover, the coherent $L1_2$ phase exhibits excellent thermal stability, which enables the hinderance of dislocation motion at elevated temperatures via the wrapping and cutting mechanisms of dislocations. The synergistic effect of nanotwins and nano-precipitates results in more significant strengthening behavior in the nanotwinned NiCo-based alloys under high temperatures. In addition, the high-temperature mechanical behavior of nanotwinned NiCo-based alloys with nano-precipitates is sensitive to the size and volume fraction of the microstructures. These findings could be helpful for the design of nanotwins and nano-precipitates to improve the high-temperature mechanical properties of NiCo-based alloys.

Keywords: NiCo-based alloys, high temperature, nano-precipitate, nanotwins, molecular dynamics simulation, mechanical behavior, deformation mechanism, dislocations

PACS: 62.20.F–, 61.72.Mm, 68.35.bd, 02.70.Ns **DOI:** 10.1088/1674-1056/ad6cca

1. Introduction

With the increasing demand for materials that exhibit superior performance under extreme conditions, the deformation behavior and mechanical properties of metallic materials at elevated temperatures have garnered significant attention in recent years.[1–3] It has been proved that high-entropy alloys (HEAs) and multi-principal element alloys (MEAs) possess better mechanical properties and demonstrate outstanding performances in high-temperature environments.[4–7] For example, the high-temperature performance of NiCo-based alloys containing nano-precipitates has been under continuous scrutiny.[8–11] In nickel-based high-entropy alloys, the addition of a certain amount of Al elements, followed by appropriate annealing treatment, can result in the formation of a highly stable $L1_2$ precipitate, Ni_3Al, within the alloy, which remains stable at high temperatures. These precipitates could significantly strengthen the alloy and greatly enhance its tensile strength and creep resistance under high-temperature conditions.[12–14] Some studies also reported that introducing nanotwins into NiCo-based alloys can enhance the plastic deformation capacity of the material.[15–17] This improvement is attributed to the more effective hindrance posed by the high-density twin boundaries (TBs) on dislocation motion.[18–20] Concurrently, nanotwins exhibit excellent thermal stability under high-temperature conditions, contributing to the enhancement of the alloy's plastic deformation behavior during service at high temperatures.[21–23]

In the past, substantial research has been conducted using atomic-scale computational methods to explore the mechanical behavior and underlying mechanisms of nanostructured metals, such as nanotwinned metals and those containing nano-precipitates.[24–27] These studies have also discussed the interaction mechanisms between dislocations and these microstructures.[28–30] For instance, Zhu *et al.* used atomic simulations to investigate the barrier mechanism of twin boundaries against dislocations and uncovered the relationship between the width of the dislocation piled-up zone near the twin boundaries and the stretching process.[29] Atomic-scale approaches have also been used to study the mechanical properties of metals at both low and high temperatures,[23,31–33] such as Liu *et al.*, who utilized molecular dynamics (MD) to explore the tensile strength and plastic behavior of CoCrCuFeNi across different temperature regimes.[34] However, even though experimental and theoretical studies have reported the strengthening effects of combined nano-precipitates and nanotwins at room temperature in NiCo-based alloys,[35–37] there is a relative dearth of discus-

†Corresponding author. E-mail: llzhu@zju.edu.cn

© 2024 Chinese Physical Society and IOP Publishing Ltd

sion on the high-temperature mechanical properties and deformation mechanisms of nanotwinned NiCo-based alloys with nano-precipitates.

In this work, the atomic method is utilized to quantitatively investigate the mechanical properties and deformation mechanisms in NiCo-based alloys containing both Ni_3Al nano-precipitates and NiCoCr nanotwins under high temperature. By employing MD simulations, the tensile deformation behavior of nanotwinned NiCo-based alloys with nano-precipitates under different temperatures is modeled to explore the impact of high temperature on the deformation behavior and mechanical properties of such novel nanostructured NiCo-based alloys. The quantitative relationship between the temperature and the mechanical performance, such as the yield stress and flow stress, is analyzed. And the interactions among the nanotwins, $L1_2$ precipitates, and dislocation motion in the high-temperature environment, as well as their synergistic strengthening mechanisms, are discussed in detail.

2. Simulation method

The MD simulations in this work are performed using the large-scale atomic/molecular massively parallel simulator (LAMMPS),[38] in which the NiCoCrFeAl five-element EAM potential developed by Farkas and Caro is used to describe the interatomic potential.[39] In the simulated model, the nano-precipitates are supposed to locate at the twin boundaries, where the volume fraction of the precipitate is 30%, as shown in Figs. 1(a)–1(c). The total atomic number of the simulation is approximately 1110000, and its three directions adopt periodic conditions. The twin space is 11.7 nm, and the diameter of the $L1_2$ precipitate (Ni_3Al) is 6 nm. In the simulations, the temperatures are set as 823 K, 923 K, 1023 K, 1123 K, 1223 K, and 1323 K, respectively, and then held for a certain amount of time under the NPT with 0 bar pressure. The simulation cells are subjected to tensile simulation along the Z direction. The engineering strain rate for loading is 2×10^8 s^{-1}. The simulation results are processed using atomic visualization software (OVITO), and the crystal structure is analyzed by common neighbor analysis (CNA).[40]

3. Results and discussion

3.1. Deformation mechanisms at high temperature

Firstly, the MD simulation results of the tensile stress–strain curves for the nanotwinned NiCo-based alloys with 30% precipitates at various temperatures are plotted in Fig. 1(d). It can be observed that the slope of the curves in the elastic deformation stage decreases with increasing temperature, indicating that the elastic modulus softens as the temperature rises. Additionally, in these stress–strain curves, a marked drop occurs when the stress reaches its maximum value, known as the yield stress, with the corresponding strain in the MD simulation defined as the elastic limit strain. It can also be discerned from Fig. 1(d) that both the elastic limit strain and the yield stress decrease with rising temperature. On the basis of the MD simulation results, quantitative analysis of the variations in the elastic modulus, elastic limit strain, and yield stress with temperature is then conducted, as illustrated in Figs. 2(a) and 2(b). One can note from the figures that the elastic modulus consistently decreases with escalating temperature, which aligns with the reports in existing work.[41] Moreover, it can also be found from Figs. 2(a) and 2(b) that a clear linear decline in both the elastic limit strain and the yield stress with increasing temperature is evident. Finally, as depicted in Fig. 1(d), the stress–strain curves enter a relatively steady plastic deformation stage, corresponding to the plastic flow stage, following the attainment of the maximum stress.

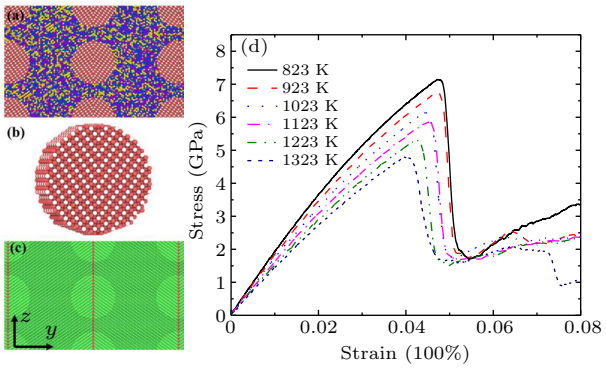


Fig. 1. The atomic composition of the MD model in which the substrate is made up of Ni, Co, and Cr; the circular portion represents the $L1_2$ precipitates (a). A detailed view of the precipitates in which the red represents Ni atoms and the white represents Al atoms (b). A lattice schematic of the alloy, wherein the green signifies the FCC structure; a single layer of red atoms represents twin boundaries (TB); the precipitate region is highlighted with brighter atoms, maintaining the FCC structure (c). The simulated stress–strain curves under tensile loading across a temperature range from 823 K to 1323 K (d).

To analyze the intrinsic mechanism behind the decrease in yield stress of the nanotwinned NiCo-based alloys with $L1_2$ nano-precipitates as the temperature increases, it can be recognized that in the MD simulations, the beginning of the yielding regime is associated with the generation of a certain volume of defects prior to plastic flow. In the yielding regime, during tensile simulations, one can primarily observe two types of defect formations: one is the formation of stacking faults, exemplified by the multiple layers of red atoms seen in Figs. 2(c) and 2(d); the other is the transformation of FCC crystal atoms into disordered atoms, represented by the white amorphous clusters in Figs. 2(e) and 2(f). To quantify the relationship between defects and yield stress, one can statistically assess the volumetric fraction of defective atoms present at the moment of yielding. Since the pre-existing amorphous atoms from the high-temperature environment do not influence the assessment, the number of disordered atoms can be subtracted before tension

from the total defect count at the point of yielding. Thereby, figure 2(b) shows the relationship between the temperature and the fraction of defective atoms produced at yielding, compared with the curve for the variation of yield strength with respect to the temperature. From the figure, it can be observed that as the temperature rises, the fraction of defective atoms increases concurrently with a decrease in yield stress. Hence, during high-temperature tensile processes, it becomes easier for defects to form, and the increased generation of these defects leads to a lower yield stress in the alloys.

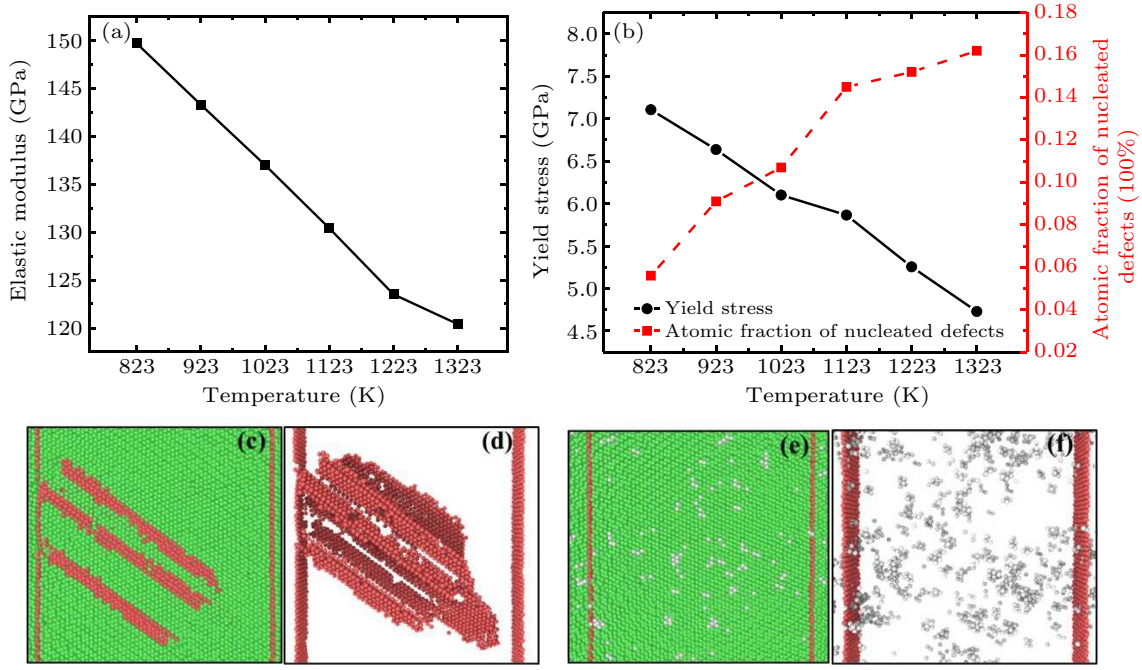


Fig. 2. The elastic modulus and elastic limit strain of the nanotwinned NiCo-based alloys with nano-precipitates varying with the temperature in the MD simulations (a); the yield stress of the nanotwinned NiCo-based alloys with nano-precipitates and the fraction of defect-forming atoms around the yielding point as functions of the temperatures (b); two primary types of defects that emerge upon yielding in the alloy (c)–(f). In (c) and (d), the red atoms represent dislocation-type defects, where (d) is a schematic of the stacking faults without the background FCC (green) atoms. In (e) and (f), the white-colored atoms indicate the structure where some atoms have transformed into an amorphous state, with (f) illustrating the matrix atoms removed from the FCC (green) background in (e). The vertical single-layer of red atoms represents the TBs.

Meanwhile, the mean flow stresses of the nanotwinned NiCo-based alloys with $L1_2$ nano-precipitates in the range of 2% plastic strain are calculated for different temperatures, as shown in curve II in Fig. 3. It can be noted from the figure that the flow stress gradually decreases as the temperature rises from 823 K to 1323K, with a plateau region observed when the temperature increases from 923 K to 1023 K. A further increase in temperature leads to a subsequent drop in the flow stress. Since the flow stress in materials is directly proportional to the density of full dislocations, as described by the Taylor model,[13] the dislocation density in the range of 2% plastic strain is examined to obtain the mean dislocation density, presented as curve I in Fig. 3. Here, it is apparent that the flow stress and mean dislocation density follow a similar trend as the temperature increases. Additionally, the variations of the flow stress with temperature for both nanotwinned NiCo-based alloys with and without nano-precipitates are plotted as curves II and III in Fig. 3, respectively. It can be discovered from the figure that the strengthening effects of the $L1_2$ nano-precipitates become remarkable with increasing temperature. This suggests that, even at high temperatures, the $L1_2$ nano-precipitates are able to keep hindering the movement of dislocations within the twin boundaries. With both precipitates and twin boundaries impeding dislocation motion, the synergistic strengthening behavior arises by accumulating more dislocations within the alloy.

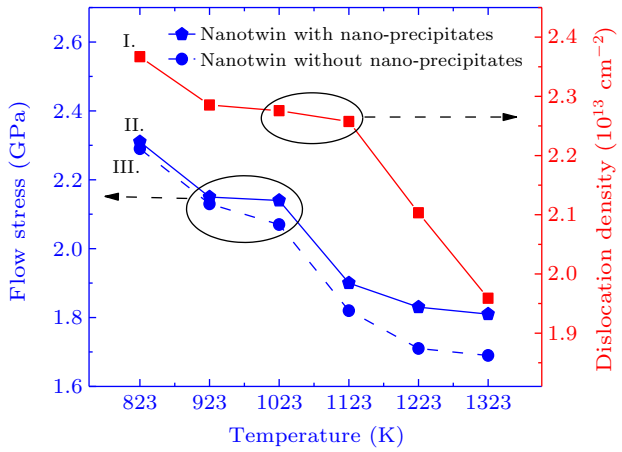


Fig. 3. The correlation between the average dislocation density and temperature during the flow stress stage is given in curve (I), compared with the average flow stress varying with the temperature in nanotwinned NiCo-based alloys with nano-precipitates in curve (II). The relationship between the average flow stress and temperature in nanotwinned NiCo-based alloys without precipitates is given in curve (III), serving as a comparison against those with precipitates.

Similar to the mechanisms observed at room temperature, there are two main modes of interaction between dislocations and precipitates: the wrapping mechanism, and the cutting mechanism. Figures 4(a)–4(c) show the wrapping mechanism observed during deformation at the temperature of 823 K. It is evident that the dislocations form distinct rings around the precipitates without further spreading, as shown in Fig. 4(c). At this point, the interior of the precipitates remains clean with no dislocations, while external dislocations are pinned outside the precipitate due to the presence of the ring-shaped dislocations, as seen in Fig. 4(b). This mechanism can increase the dislocation density within the twins to enhance the strength. Figures 4(d)–4(f) present the cutting mechanism observed during deformation at 923 K. It is equally clear from Fig. 4(e) that the dislocations cut into the precipitates and get pinned inside them. Unlike the wrapping mechanism, numerous dislocations are trapped within the precipitates in this case: see Fig. 4(f). Since the TBs within the precipitate also create obstacles to prevent the dislocation movement, there is still the pinning effect once the dislocation enters the precipitate. This could lead to an overall increase in the dislocation density within the nanotwinned NiCo-based alloys, thus augmenting the flow stress and making the material stronger.

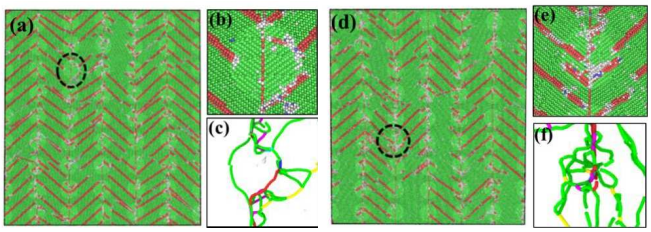


Fig. 4. The CNA analysis of the wrapping mechanism of precipitates under the temperature of 823 K, where (b) corresponds to the dashed area in (a), and (c) is the DXA analysis for (b). The CNA analysis of the cutting mechanism of precipitates under the temperature of 923 K where (e) corresponds to the dashed area in (d), and (f) is the DXA analysis for (e).

Figure 5 presents the dislocation distributions of nanotwinned NiCo-based alloys with nano-precipitates at temperatures of 823 K, 1023 K, and 1323 K, respectively, when the plastic strain is 1%. It can be found from the figure that the overall number of dislocations visibly declines as the temperature rises, corresponding to the decreasing overall flow stress. One can also observe that the wrapping mechanism becomes increasingly prevalent, while the cutting mechanism diminishes with increasing temperature. This is because, at higher temperatures, the $L1_2$ precipitates exert a stronger inhibitory effect on dislocation movement relative to the twin boundaries. According to Fig. 3, despite the downward trend of the overall flow stress between 823 K and 1323 K, the strengthening effect of the $L1_2$ precipitates becomes more pronounced. This enhanced reinforcement is attributed to the more prominent strengthening role played by the wrapping mechanism around the precipitates, as shown in Fig. 5. Therefore, it can be concluded that within the temperature range of 823 K to 1323 K, the synergistic strengthening behavior occurs as a result of the nano-precipitates and nanotwins in NiCo-based alloys.

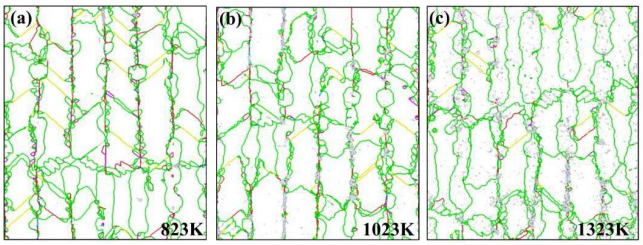


Fig. 5. The dislocation distributions in nanotwinned NiCo-based alloys with nano-precipitates after 1% plastic strain at the temperatures of 823 K (a), 1023 K (b), and 1323 K (c).

3.2. Mechanical performance with various sizes and volume fractions of microstructures

Since the geometrical size and volume fraction of microstructures can affect the mechanical performance of nanostructured metallic materials significantly,[42–46] further MD simulations are conducted to explore the high-temperature mechanical performance of nanotwinned NiCo-based alloys with nano-precipitates for various sizes and volume fractions of nanotwins and nano-precipitates. Figure 6 shows the effect of the volume fraction of nano-precipitates on the mechanical performance of nanotwinned NiCo-based alloy at high temperatures. The stress–strain curves for the volume fractions of 10% and 20% are plotted in Figs. 6(a) and 6(b), respectively. By combining with Fig. 1(d), one can obtain the yield stress and flow stress varying with temperature for different volume fractions of nano-precipitates, as presented in Figs. 6(c) and 6(d), respectively. It is found in the figures that both the yield stress and flow stress are weakened as the temperature increases, and the volume fraction can change the dependence of these mechanical properties on temperature. In Fig. 6(c), it can be observed that up to 1023 K, the changes in the yield stress with volume fractions are not significant. With a further increase in temperature, the dependence of the yield stress on the volume fraction becomes more pronounced at higher temperatures. In Fig. 6(d), within the temperature range of 823 K to 1323 K, one can see that as the volume fraction of the precipitates decreases, the flow stress increases. Additionally, the flow stress becomes more sensitive to the temperature in the lower volume fraction of nano-precipitates.

The high-temperature mechanical properties of nanotwinned NiCo-based alloys for different sizes of nano-precipitates are also simulated and plotted in Fig. 7. The stress–strain curves for the nano-precipitate diameters of 3 nm and 9 nm are given in Figs. 7(a) and 7(b), respectively. Similarly, by combining with Fig. 1(d), one can achieve the yield stress and flow stress of nanotwinned NiCo-based alloys as

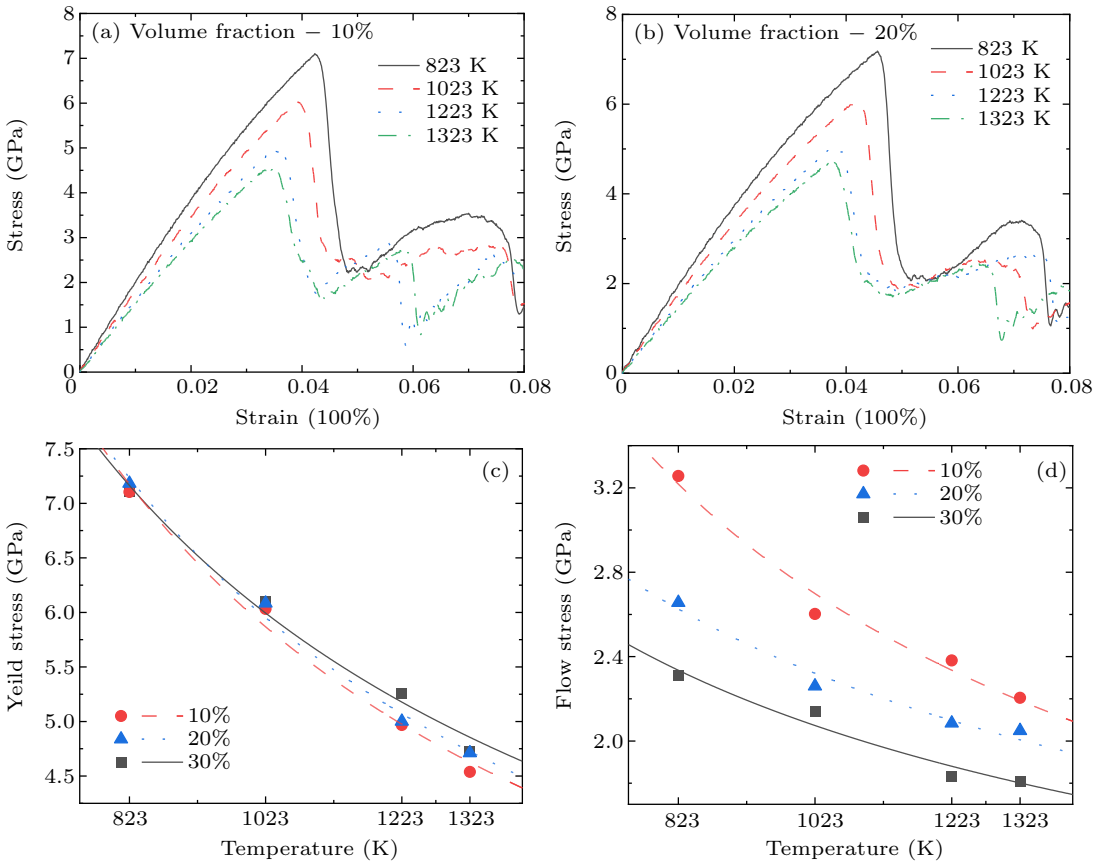


Fig. 6. The stress–strain curves for the volume fractions of Ni_3Al nano-precipitates of 10% (a) and 20% (b), and the yield stress (c) and flow stress (d) varying with the temperature for the volume fractions of Ni_3Al nano-precipitates of 10%, 20%, and 30%.

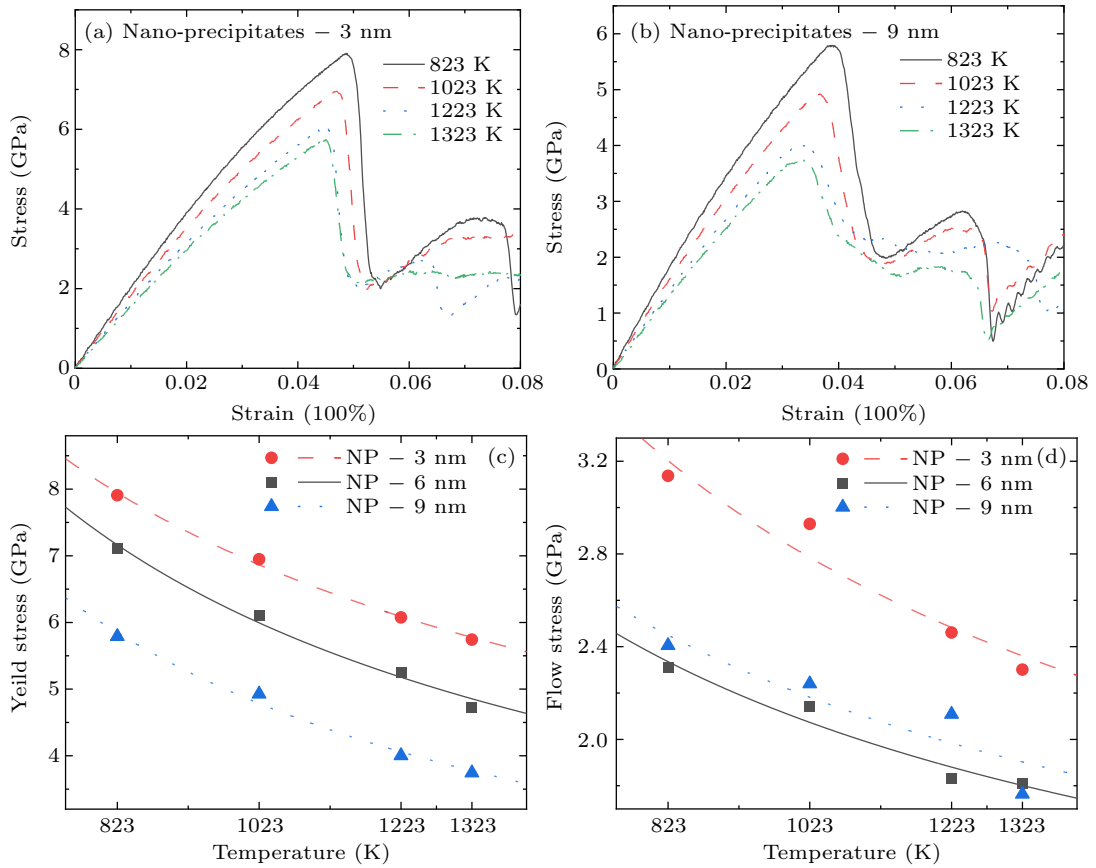


Fig. 7. The stress–strain curves for the diameters of Ni_3Al nano-precipitates of 3 nm (a) and 9 nm (b), and the yield stress (c) and flow stress (d) varying with the temperature in the Ni_3Al nano-precipitates of 3 nm, 6 nm and 9 nm.

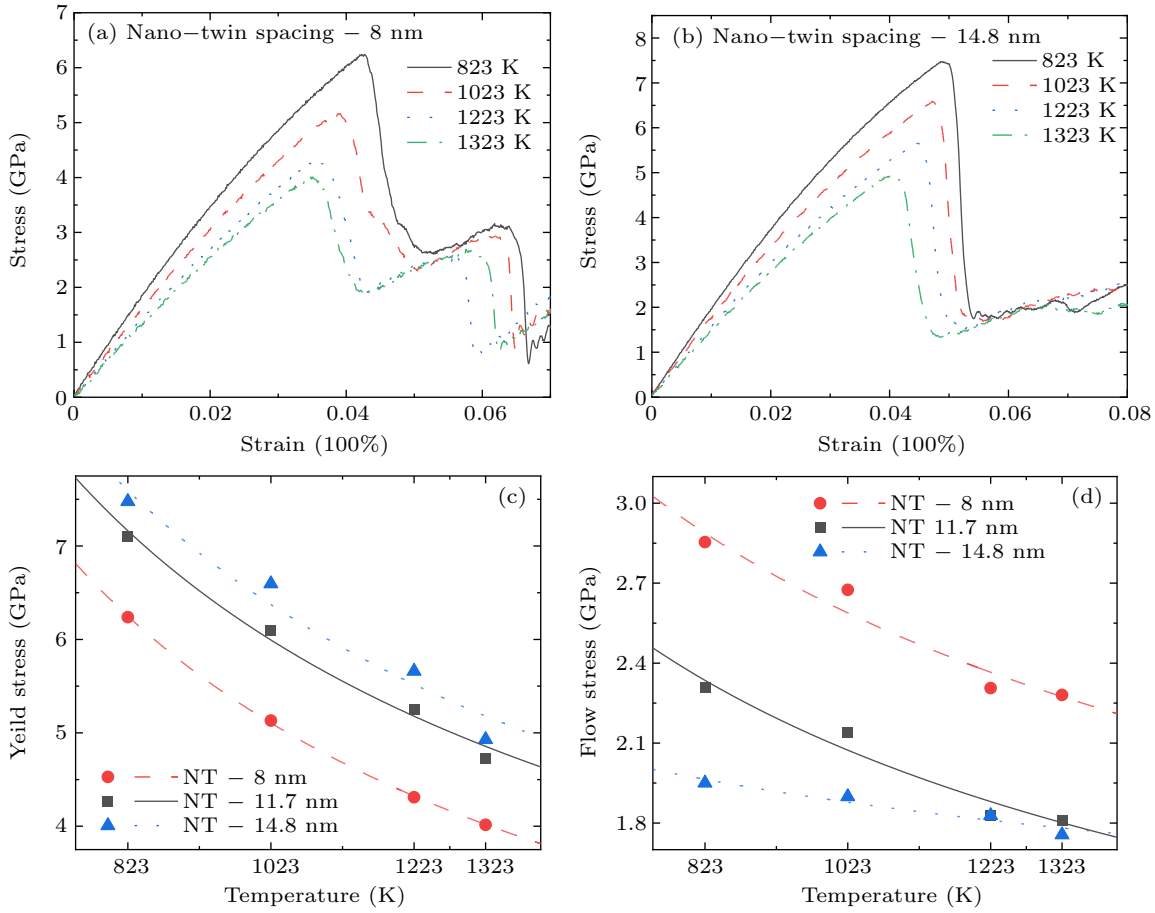


Fig. 8. The stress–strain curves for the twin spacing of 8 nm (a) and 14.8 nm (b) with the volume fraction of 6 nm-Ni_3Al nano-precipitates, and the yield stress (c) and flow stress (d) varying with temperature for the twin spacings of 8 nm, 11.7 nm and 14.8 nm.

functions of temperature for different nano-precipitate sizes, as shown in Figs. 7(c) and 7(d), respectively. It can be seen in Fig. 7(c) that within the temperature range of 823 K to 1323 K, the yield stress decreases as the size of the precipitates increases. In Fig. 7(d), one can find that the flow stress is the highest for the precipitate size of 3 nm, is the lowest for 6 nm, and then rises slightly for 9 nm. This is because the volume fraction of 3 nm sized nano-precipitates is much lower than those for the 6 nm and 9 nm sized nano-precipitates, leading to the higher flow stress, as shown in Fig. 6(d). It can also be suggested from Fig. 7(d) that there should be a critical diameter of precipitates between 3 nm and 9 nm to achieve the minimum flow stress in nanotwinned NiCo-based alloys for a given twin spacing. Figure 8 further discusses the influence of twin spacing on the high-temperature mechanical properties of nanotwinned NiCo-based alloys with nano-precipitates. Figures 8(a) and 8(b) depict the stress–strain curves of nanotwinned NiCo-based alloys with nano-precipitates for the twin spacings of 8 nm and 14.8 nm, respectively. Then, one can obtain the yield stress and flow stress varying with the temperature for different twin spacings by combining Figs. 1(d), 8(a) and 8(b). It can be seen in Fig. 8(c) that within the temperature range of 823 K to 1323 K, the yield stress of the alloys also increases as the twin spacing increases. Conversely, it is clearly shown in Fig. 8(d) that the flow stress decreases as the twin spacing increases. This aligns with the well-established phenomenon that the strengthening effect increases as the twin spacing decreases due to the excellent thermal stability of nanotwins.[47,48]

4. Conclusion

In summary, atomic simulations were performed to monitor the effects of nanotwins and nano-precipitates on the high-temperature mechanical properties and strengthening mechanisms in NiCo-based alloys. The molecular dynamic simulations revealed that the proliferation of defective atoms at the onset of yielding makes the yield stress decrease when the temperature increases. The decrement of the flow stress in nanotwinned NiCo-based alloys with nano-precipitates with the higher temperature comes from the variation of dislocation density with the temperature. Furthermore, the nano-precipitates could enhance the high-temperature strengthening behavior in nanotwinned NiCo-based alloys. This stems from the dislocation interactions with both the nanotwins and the nano-precipitates, including the wrapping and cutting behavior of dislocations. As the temperature increases, the ten-

dency for dislocation wrapping increases while cutting activity diminishes, suggesting that dislocation wrapping provides a more pronounced strengthening contribution. The results of MD simulations also demonstrated that a higher yield stress can be achieved for a higher volume fraction of precipitates, a smaller nano-precipitate size and larger twin spacing. Enhanced flow stress can be obtained for the lower volume fraction of precipitates, the smaller nano-precipitate size and the smaller twin spacing. The findings in this work could be helpful for the optimization of nanotwins and nano-precipitates to improve the high-temperature mechanical performance of NiCo-based alloys.

Acknowledgments

Project supported by the National Natural Science Foundation of China (Grant No. 12072317) and the Natural Science Foundation of Zhejiang Province (Grant No. LZ21A020002). Ligang Sun gratefully acknowledges the support received from the Guangdong Basic and Applied Basic Research Foundation (Grant No. 22022A1515011402), the Science, Technology and Innovation Commission of Shenzhen Municipality (Grant No. GXWD20231130102735001), and Development and Reform Commission of Shenzhen (Grant No. XMHT20220103004).

References

[1] Juan C C, Tsai M H, Tsai C W, *et al.* 2015 *Intermetallics* **62** 76
[2] Maresca F and Curtin W A 2020 *Acta Mater.* **182** 235
[3] Wang M L, Lu Y P, Lan J G, *et al.* 2023 *Acta Mater.* **248** 118806
[4] Gludovatz B, Hohenwarter A, Catoor D, *et al.* 2014 *Science* **345** 1153
[5] Gludovatz B, Hohenwarter A, Thurston K V S, *et al.* 2016 *Nat. Comm* **7** 10602
[6] Diao H Y, Feng R, Dahmen K A and Liaw P K 2017 *Curr. Opin. Solid ST. M.* **21** 252
[7] Guo Y N, Su H J, Zhou H T, *et al.* 2022 *J. Mater. Sci. Technol.* **111** 298
[8] Wu Z, Bei H, Pharr G M and George E P 2014 *Acta Mater.* **81** 428
[9] Schneider M, George E P, Manescau T J, *et al.* 2020 *Int. J. Plasticity* **124** 155
[10] Verma A, Tarate P, Abhyankar A C, *et al.* 2019 *Scr. Mater.* **161** 28
[11] Li W J and Wang C Y 2020 *Chin. Phys. B* **29** 026102
[12] Zhang Z J, Sheng H W, Wang Z J, *et al.* 2017 *Nat. Commun.* **8** 14390
[13] Ding L, Hilhorst A, Idrissi H and Jacques P J 2022 *Acta Mater.* **234** 118049
[14] Li Z, Hu Y, Li X, *et al.* 2023 *Compos. Pt. B-Eng.* **265** 110965
[15] Fan J, Ji X, Fu L, *et al.* 2022 *Int. J. Plasticity* **157** 103398
[16] Zhu Z Y, Yan S H, Chen H and Gou G Q 2021 *Mater. Sci. Eng. A* **803** 140501
[17] Zhang T W, Ma S G, Zhao D, *et al.* 2020 *Int. J. Plasticity* **124** 226
[18] Liu X W, Sun L G, Zhu L L, *et al.* 2018 *Acta Mater.* **149** 397
[19] Chen A Y, Zhu L L, Sun L G, *et al.* 2019 *Nat. Comm.* **10** 1403
[20] Wu G, Chan K C, Zhu L L, Sun L G and Lu J 2017 *Nature* **545** 80
[21] Chen G, Peng Y, Zheng G, *et al.* 2016 *Nat. Mater.* **15** 876
[22] Edwards T E J, Rohbeck N, Huszár E, *et al.* 2022 *Adv. Sci.* **9** 2203544
[23] He X, Xu Z Y and Ni Y S 2024 *Chin. Phys. B* **33** 016201
[24] Barrett C D, Tschopp M A and El Kadiri H 2012 *Scr. Mater.* **66** 666
[25] An M R, Song H Y and Su J F 2012 *Chin. Phys. B* **21** 106202
[26] Zhang Z Y, Wang B, Huang S L, *et al.* 2016 *Mater. Des.* **106** 313
[27] Fan H D, Zhu Y X, El-Awady J A and Raabe D 2018 *Int. J. Plasticity* **106** 186
[28] Chen Y, Fang Q, Luo S, *et al.* 2022 *Int. J. Plasticity* **155** 103333
[29] Zhu L, Ruan H, Li X, *et al.* 2011 *Acta Mater.* **59** 5544
[30] Tian Y Y, Luo G J, Fang Q H, Li J and Peng J 2022 *Chin. Phys. B* **31** 066204
[31] Sun Z H, Zhang J, Xin G X, *et al.* 2022 *Intermetallics* **142** 107444
[32] Afkham Y, Bahramyan M, Mousavian R T and Brabazon D 2017 *Mater. Sci. Eng. A* **698** 143
[33] Xie L, Brault P, Thomann A L, Bauchire J M, *et al.* 2013 *Appl. Surf. Sci.* **285** 810
[34] Liu J 2020 *Phys. Lett. A* **384** 126516
[35] Zhang H, Ren Z Y, Tong Y G, *et al.* 2023 *J. Mater. Sci. Technol.* **156** 172
[36] Zhang H, Tong Y G, Cao S H, *et al.* 2022 *J. Alloys Compd.* **919** 165715
[37] Liu L Y, Zhang Y, Ma J M, *et al.* 2022 *Scr. Mater.* **217** 114771
[38] Thompson A P, Aktulga H M, *et al.* 2022 *Comput. Phys. Commun.* **271** 108171
[39] Farkas D and Caro A 2020 *J. Mater. Res.* **35** 3031
[40] Zhang J, Ma S H, Xiong Y X, *et al.* 2021 *Acta Mater.* **219** 117238
[41] Liu R G, Tang J, Jiang J X, *et al.* 2022 *Extreme Mech. Lett.* **56** 101875
[42] Sun L G, Wu G, Wang Q and Lu J 2020 *Mater. Today* **38** 114
[43] An M R, Lei Y F, Su M J, *et al.* 2023 *Chin. Phys. B* **32** 066201
[44] Jiao L, Zhu L, Gan B, *et al.* 2023 *Mech. Mater.* **186** 104806
[45] Zhou M, Wang W, Su H J, *et al.* 2024 *Chin. Phys. B* **33** 056501
[46] Xing R L and Liu X P 2024 *Chin. Phys. B* **33** 016202
[47] Zhang B B, Yan F K, Zhao M J, *et al.* 2018 *Acta Mater.* **151** 310
[48] Sun L G, Li D, Zhu L, *et al.* 2020 *Int. J. Plasticity* **128** 102685